Behavior of geopolymer and conventional concrete beam column joints under reverse cyclic loading

S. Deepa Raj[*1], N. Ganesan[2a], Ruby Abraham[3] and Anumol Raju[1]

[1]*Department of Civil Engineering, College of Engineering Trivandrum, Kerala, India*
[2]*Department of Civil Engineering, National Institute of Technology, Calicut, Kerala, India*
[3]*Rajiv Gandhi Institute of Technology, Kottayam, Kerala, India*

Abstract. An experimental investigation was carried out on the strength and behavior plain and fiber reinforced geopolymer concrete beam column joints and the results were compared with plain and steel fiber reinforced conventional concrete beam column joints. The volume fraction of fibers used was 0.5%. A total of six Geopolymer concrete joints and four conventional concrete joints were cast and tested under reversed cyclic loading to evaluate the performance of the joints. First crack load, ultimate load, energy absorption capacity, energy dissipation capacity stiffness degradation and moment-curvature relation were evaluated from the test results. The comparison of test results revealed that the strength and behavior of plain and fiber reinforced geopolymer concrete beam column joints are marginally better than corresponding conventional concrete beam column joints.

Keywords: fiber; geopolymer; alkaline solution; energy dissipation; stiffness degradation

1. Introduction

The major issue facing the construction industry at present is the need for environmental friendly construction materials for sustainable development. The main ingredient of conventional concrete is Ordinary Portland cement (OPC). The manufacture of cement is leading to the depletion of natural resources like limestone and causes environmental pollution due to the emission of carbon dioxide (CO_2) (Bakri *et al.* 2011). Geopolymers are alternative binders to cement. It is a type of alumino-silicate product, produced by chemical activation of molecules which are rich in alumina and silica. Concrete made using geopolymers as binders is called geopolymer concrete (GPC). Fly ash based geopolymer concrete has pozzolanic properties similar to OPC based conventional concrete. Since it uses waste material like fly ash as the main ingredient, it can be regarded as a sustainable green material (Hardjito *et al.* 2004). Studies conducted on the material properties of GPC showed that it has better engineering properties and durability characteristics than conventional concrete (Ganesan *et al.* 2015, Rangan 2006, Bakharev 2005, Sarker 2011). The structural behavior of geopolymer concrete columns subjected to axial

---

compressive loading and uniaxial bending were studied by various researchers (Sujatha *et al.* 2012, Sarker 2009) and found that GPC columns exhibited higher load carrying capacity and less deformation than corresponding conventional concrete (CC) columns.

The studies on structural behavior of GPC beams indicated better performance and enhanced load carrying capacity and flexural strength than conventional concrete beams (Kannapiran *et al.* 2013, Dattatreya 2011).

The design of reinforced concrete structures with high ductility gained importance due to the frequently occurring earthquakes in different parts of the world. Since beam column joints are the vulnerable locations of structural system, strength and ductility of structures depend mainly on the proper detailing of reinforcement in beam-column joints. Joints get severely damaged when they are subjected to forces larger than the design force in cyclic manner during earthquakes. Beam column joints in a reinforced concrete moment resisting frame are crucial zones for transfer of loads effectively between the connecting elements of the structure (Ganesan *et al.* 2014, Haach *et al.* 2008). The flow of forces within a beam-column joint may be interrupted if the shear strength of the joint is not adequate. Under seismic excitations, the beam-column joint region is subjected to horizontal and vertical shear forces whose magnitudes are many times higher than those within the adjacent beams and columns. Fiber reinforced concrete resist more cycles of loading even after cracking. Addition of steel fibers would improve toughness, energy dissipation capacity and damage tolerance of concrete, which are most important characteristics for structures under seismic loading (Ganesan *et al.* 2014, Haach *et al.* 2008).

The experimental investigations on the structural behavior of conventional concrete beam column joints showed that the strength of a joint depends on factors such as detailing of reinforcement, bond strength, spacing of connecting ties, geometry of beam and column, strength of concrete, column axial load and percentage of fibers (Ganesan *et al.* 2014, Haach *et al.* 2008). Even though large number of studies have been conducted to understand the mechanical properties of GPC, attempts on the investigation of geopolymer concrete beam column joints have not been come across so far.

2. Experimental programme

The experimental programme consists of casting and testing of plain and fiber reinforced (0.5% volume fraction of fibers) GPC exterior beam column joints (GBJ) and conventional concrete beam column joints (CCJ) under reverse cyclic loading.

2.1 Materials used

Ingredients of GPC were low calcium fly ash (Class F), coarse aggregate, fine aggregate, alkaline solution and superplasticiser. Crushed granite stones having nominal size 20 mm and natural river sand were used as coarse aggregate and fine aggregate respectively. Both the coarse and fine aggregate used were conforming to Zone II of IS 383(1970). The material properties of coarse and fine aggregates are shown in Table 1. A mixture of sodium silicate solution with SiO_2 to Na_2O ratio by mass of 2 (Na_2O=14.7%, SiO_2=29.4%) and water=55.9% and sodium hydroxide solution was chosen as the alkaline liquid to activate the source material. The sodium hydroxide solution was prepared by mixing sodium hydroxide pellets in water. A naphthalene based superplasticizer was also added to make the concrete workable. Ordinary Portland cement of

Table 1 Properties of coarse and fine aggregates

Parameters	CA	FA
Nominal maximum size	20 mm	4.75 mm
Specific gravity	2.89	2.24
Bulk density (g/cc)	1.54	1.23
Void ratio	0.86	0.81
Fineness modulus	7.00	3.85

Table 2 Mix proportion of GPC and CC

Constituent Material	Quantity (kg/m^3)	
	GPC	CC
Fly ash	408.0	-
Sodium Silicate	103.0	-
Sodium hydroxide	41.0	-
Coarse aggregate	1248.0	1266
Fine aggregate	600.0	598
Water	14.5	192
Superplasticiser	10.2	-
Cement	-	360

53 grade conforming to IS: 12269 (1987) was used for preparing conventional concrete. Hooked end steel fibers with aspect ratio 60 (length 30 mm and diameter 0.5 mm) were used to prepare the steel fiber reinforced concrete mix.

2.2 Mix design

As GPC is a recently developed construction material, no standard mix design procedures are available so far. Therefore GPC mix of M30 grade was designed by performing various trials as per the guidelines proposed by Rangan (2006). The final mix proportion was selected based on compressive strength and workability and is given in Table 2. The mix design for M30 grade conventional concrete (CC) was also done as per IS 10262(2009) and the final mix proportion selected is given in Table 2. For preparing fiber reinforced specimens, 0.5% volume fraction of hooked end steel fibers were added to GPC and CC mix and are designated as SFRGPC and SFRC respectively.

2.3 Details of specimens

The cross sections of beam and column are 150 mm×200 mm and 200 mm×200 mm respectively. The column was reinforced with four 10 mm diameter high yield strength deformed (HYSD) bars and the beam was provided with two 10 mm diameter HYSD bars each at top and bottom. HYSD bars of 6 mm diameter were used as transverse ties in column and stirrups in beam. The overall
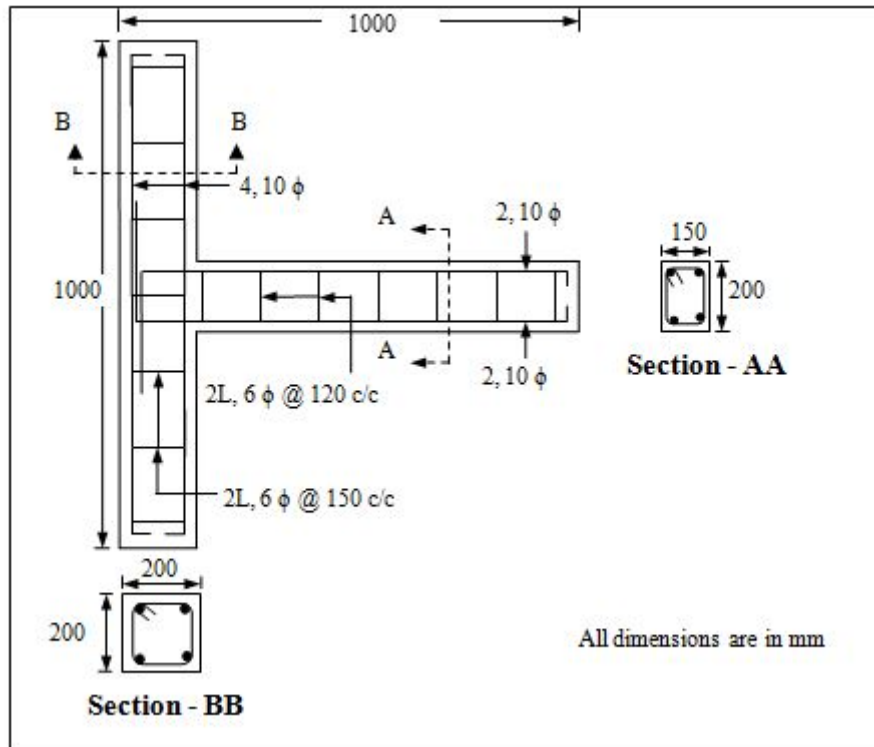
Fig. 1 Dimension and reinforcement details of specimens

dimensions and reinforcement details of joint specimens are shown in Fig. 1. Geopolymer and conventional concrete beam column joints are designated as GBJ and CCJ respectively. Fiber reinforced geopolymer concrete and conventional concrete beam column joints are designated as SFRGBJ and SFRCCJ respectively.

2.4 Preparation of specimens

The coarse aggregate and fine aggregate in saturated surface dry condition were mixed in a laboratory pan mixer with fly ash for three minutes. Then alkaline solutions, superplasticiser and extra water were added to the dry materials and mixed for four minutes. For fiber reinforced specimens, fibers were added to the dry materials and mixed for three minutes and then the alkaline solutions and super plasticiser were added and mixed for four minutes. The workability of fresh concrete was determined by conducting slump and compacting factor test and the results are given in Table 3. All beam column joints were cast horizontally and concrete was poured in moulds in 5 cm layers and compacted using a needle vibrator. The fiber reinforced joints (SFRGBJ and SFRCCJ) were cast with fiber volume fraction of 0.5%. In order to determine the hardened properties, standard cubes of size 150 mm, cylinders of 150 mm diameter and 300 mm height and prisms of size 100 mm×100 mm×500 mm were cast. After casting, geopolymer concrete specimens were covered with polythene sheets to prevent loss of moisture and kept at room temperature for one day. For GPC, no water curing is required and heat curing for one day is sufficient (Hardjito *et al*. 2004).

Table 3 Fresh and hardened properties of GPC and CC

Mix	GPC	CC	SFRGPC	SFRCC
Slump (mm)	90	92	78	80
Compacting factor	0.90	0.92	0.80	0.86
Compressive strength (N/mm^2)	34	35	37.2	38.5
Split tensile strength (N/mm^2)	3.86	3.25	4.20	3.60
Flexural strength (N/mm^2)	4.10	3.77	4.57	4.20
Modulus of elasticity (N/mm^2)	38148	26678	40156	30149
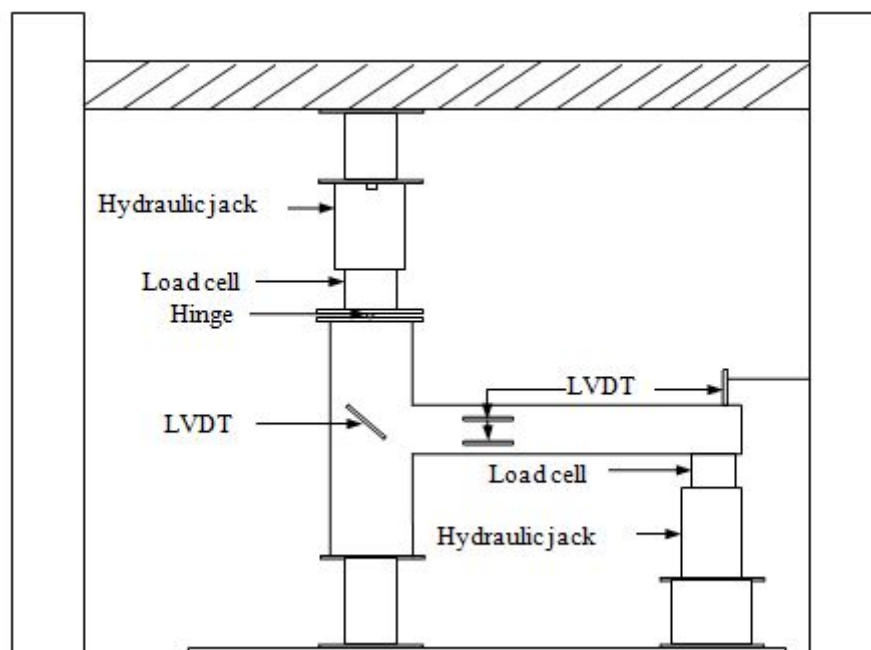
Fig. 2 Schematic diagram of test setup

The GPC specimens were placed along with moulds inside the oven and cured at 600C for 24 hours. After curing, the specimens were removed from the chamber and left to air-dry at room temperature for another 24 hours before demoulding. Tests were conducted to evaluate the hardened properties such as compressive strength, split tensile strength, flexural strength and modulus of elasticity of plain and fiber reinforced GPC and CC specimens and the results are given in Table 3.

2.5 Testing of specimens

The specimens after 28 days of casting were tested in an upright position in a loading frame. The bottom end of the column was simply supported and the top end was provided with a hinged support, which was simulated by a steel ball placed between the grooves of two steel plates. An axial compressive load equal to 20% of the load carrying capacity of the column was applied on the column by means of a hydraulic jack of capacity 1000 kN so as to make it stable. The beam

Fig. 3 Test setup

(a)

(b)

(c)

(d)
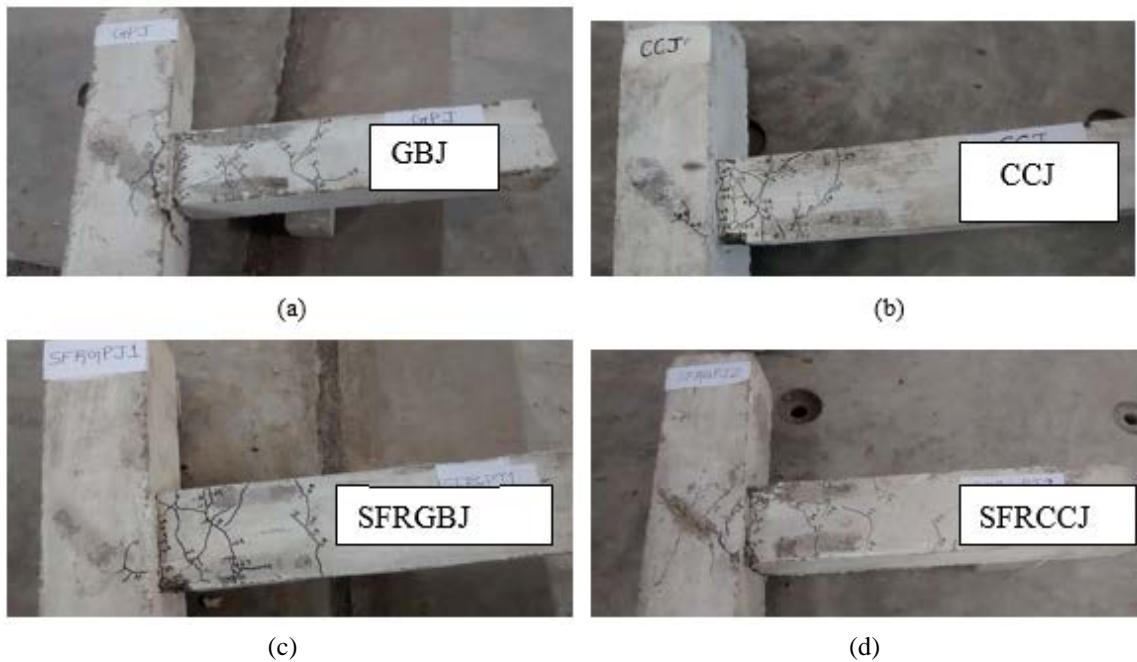
Fig. 4 Crack pattern of specimens

end was subjected to reverse cyclic loading using 200 kN hydraulic jack connected to the load cell through the plunger of the jack. LVDTs having least count of 0.1 mm and 100 mm travel was placed at the beam end to measure the deflections at beam tip. The strains at the extreme compression and tension fibers of beam were recorded using LVDTs of 0.01 mm least count and 50 mm travel as shown in Fig. 2. The photograph of the test setup is shown in Fig. 3. Each cycle of loading consists of a forward cycle and a backward cycle. For the first forward cycle, specimens were loaded up to 1 kN and then unloaded to zero. For the backward cycle, the specimens were loaded to 1 kN in the negative direction and unloaded to zero so that a full cycle of reverse cyclic loading could be obtained. For the second cycle, specimens were loaded up to 2 kN, then unloaded

to zero and in the backward cycle it was loaded in the negative direction to 2 kN and unloaded to zero. This procedure was repeated for 3 kN, 4 kN etc. till the failure of the joints. Deflection at beam tip and readings of LVDT's placed at the top and bottom were measured at each cycle of loading at 1 KN intervals. The width of cracks was also measured at regular intervals using crack detection microscope with a least count of 0.02 mm up to 0.3 mm crack width.

2.6 Failure pattern

Fig. 4 shows the crack pattern of the plain (Figs. 4(a) and 4(b)) and fiber reinforced (Figs. 4(c) and 4(d)) GBJ and CCJ specimens. In all specimens, the cracks appeared near the joint after the first crack load. With further increase of loading, the cracks propagated up to the beam top and initial cracks started widening at the bottom. Cracks were initiated and widened at the top of beams during the backward cycle of loading. Finally the cracks widened leading to the failure of the joint at the beam bottom. Most of the cracks were concentrated in the beam portion near the joint. Micro cracks were observed in the joint region during the test and joint shear failure did not occur in all the specimens. The failure of the joint was due to the crushing of concrete at the beam during the forward cycle of loading. The behavior of SFRGBJ and SFRCCJ were almost similar. GBJ and CCJ specimens were observed to have wider cracks when compared to the fiber reinforced specimens. In the case of SFRGBJ and SFRCCJ specimens, more number of finer cracks were formed. This can be attributed to the effect of steel fibers to control the cracks at both micro and macro level.

(a) GBJ   (b) CCJ

(c) SFRGBJ   (d) SFRCCJ
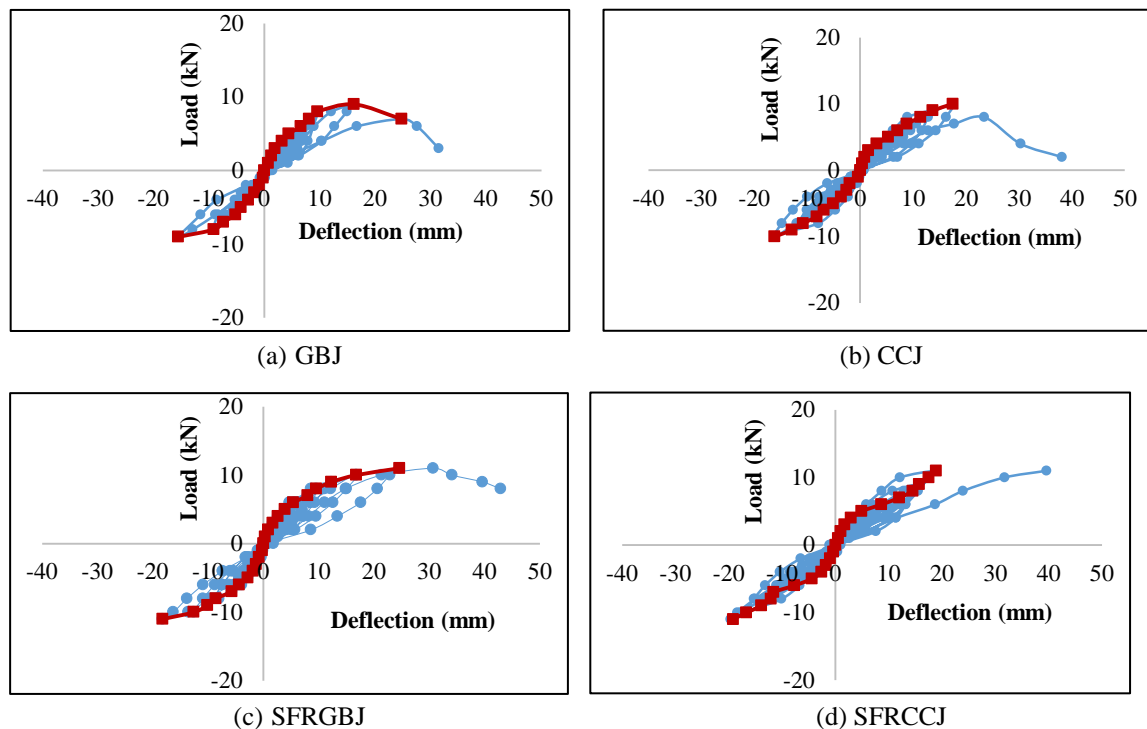
Fig. 5 Load-deflection curves
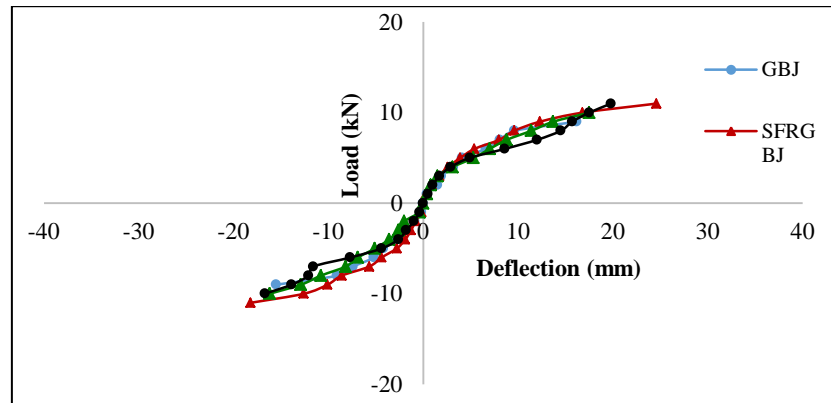
Fig. 6 Load-deflection envelope curves

Table 4 First crack load and ultimate load

Specimen	First crack load (kN)	Ultimate load (kN)
GBJ	3.0	9.0
SFRGBJ	4.0	11.0
CCJ	3.0	10.0
SFRCCJ	3.5	11.0

3. Results and discussions

3.1 Load-deflection behavior

From the recorded values of load and deflections for each cycle of loading, the load-deflection hysteresis curves were plotted for plain and fiber reinforced GBJ and CCJ and are shown in Fig. 5. In both GBJ and CCJ specimens, the joints failed in the last forward cycle of loading with excessive deflections. Envelope curves were obtained by joining the peak points of all the cycles and are shown in Fig. 6. From the Figure it may be noted that deflection of the joint until the initiation of cracks increased linearly and was proportional to the load. After the initial cracking, deflection increased nonlinearly until the maximum load was reached. It can also be inferred from the envelope curve that GBJ and CCJ specimens showed almost similar behavior. Addition of steel fibers enhanced the load deflection behavior of both GBJ and CCJ. The presence of steel fibers improved the strength and behavior of both GBJ and CCJ.

3.2 First crack load and ultimate load

First crack load was determined from the envelope curve of the load deflection plot corresponding to the point at which the curve deviated from linearity. The first crack load of all the tested specimens are given in Table 4. From the table it can be observed that the first crack load of GBJ and CCJ are same. But the addition of fibers improved the first crack load, which may be due to the increase in tensile strain carrying capacity of concrete in the neighbourhood of fibers. The first crack load increased by 33.33% for SFRGBJ and 16.7% for SFRCCJ. The values of

Table 5 Energy absorption capacity

Specimen	Energy absorption capacity(kNmm)	
	Forward cycle	Backward cycle
GBJ	101.9	-100.05
SFRGBJ	196.8	-142.7
CCJ	114.25	-101.4
SFRCCJ	119.15	-103.15

Table 6 Displacement ductility of GBJ and CCJ

Specimen	Yield deflection (δ_y) (mm)	Ultimate deflection (δ_u) (mm)	Displacement ductility	
			Absolute (δ_u/δ_y)	Relative
GBJ	4.4	16.2	3.68	1.47
SFRGBJ	5.4	24.6	4.56	1.82
CCJ	7.0	17.5	2.50	1.00
SFRCCJ	4.9	18.9	3.86	1.54

ultimate load of tested specimens are given in Table 4. Addition of steel fibers in the concrete increased the ultimate load carrying capacity of the joints, due to the bridging of micro cracks by steel fibers. The ultimate load of SFRGBJ is 22% greater than GBJ whereas for SFRCCJ it is 10% greater than CCJ.

3.3 Energy absorption capacity and ductility

The area under the load deflection curve indicates the energy absorption capacity. The energy absorption capacity of GBJ and CCJ are given in Table 5. From the table it is clear that the energy absorption capacity of GBJ and CCJ are almost the same. As fibers are introduced into concrete, energy absorption capacity of both GBJ and CCJ increased in a similar manner. For both specimens, the forward cycle had a higher energy absorption capacity than backward cycle. Earthquake resistant structures should be capable of deforming in a ductile manner when subjected to cyclic loading. Ductility of a structure is its ability to undergo deformation beyond the initial yield deformation, while still sustaining the load. The ductility factor, which is a measure of ductility of a structure is defined as the ratio of maximum deflection (δ_u) to the deflection at yield (δ_y). Displacement ductility is adopted to make a quantitative assessment of ductility enhancement. Displacement ductility of GBJ was 1.47 times higher than that of CCJ. This may be due to the difference in microstructure between Geopolymer concrete and conventional concrete. The higher value of displacement ductility of GBJ indicates that the use of geopolymer as constituent material makes the member more ductile than CCJ. The increased ductility of GBJ than CCJ points validates the superior behavior of GBJ under cyclic loading. Table 6 depicts the displacement ductility of the specimens.

3.4 Energy dissipation capacity

Energy-dissipation capacity is an important indicator of the seismic properties of a structure. A
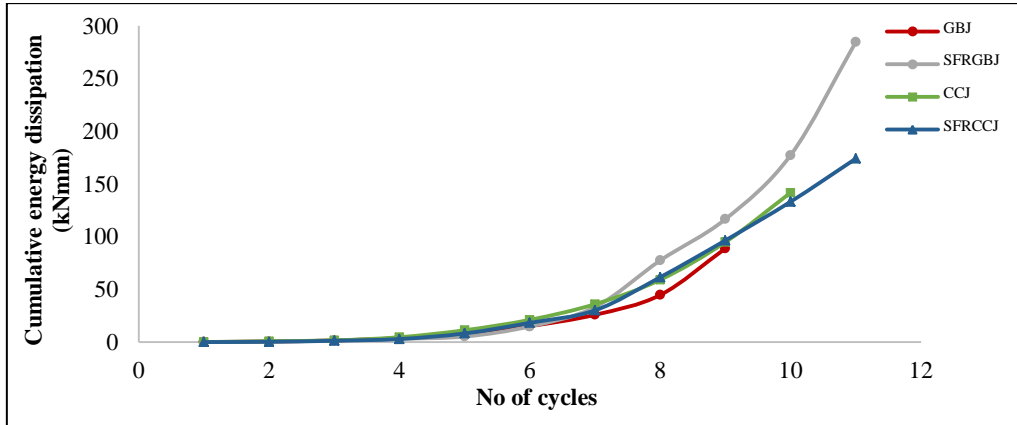
Fig. 7 Cumulative energy dissipation
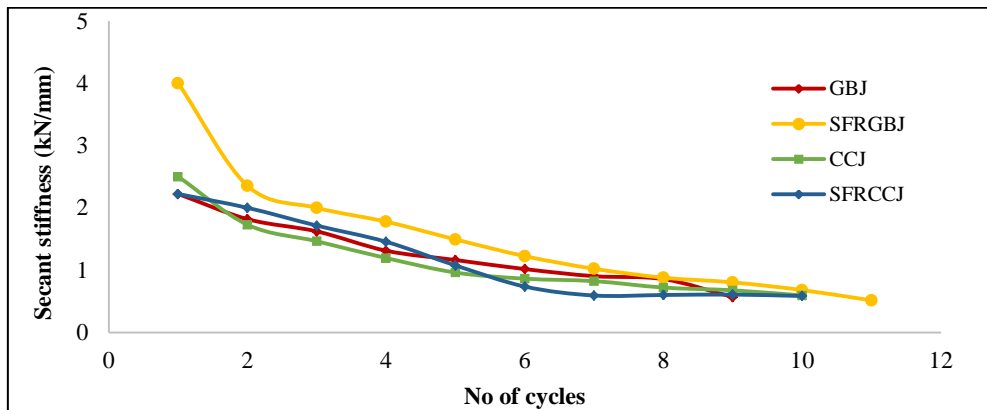
Fig. 8 Stiffness degradation

structure can withstand strong ground earthquake motions only if it has sufficient ability to dissipate seismic energy. It is the area within the load-deflection hysteretic loop for every cycle of load. The cumulative energy dissipated by the specimens was calculated by summing up the energy dissipated in consecutive load displacement loops throughout the test. The cumulative energy dissipation of the specimens during each cycle is shown in Fig. 7. From the graph, it may be seen that the increase in energy dissipation after each cycle for GBJ and CCJ specimens are comparable and the curves show a similar trend. GBJ and CCJ had comparable values of cumulative energy dissipation and the energy dissipation capacity increased with addition of steel fibres. The cumulative energy dissipation of SFRGBJ was 39% higher than SFRCCJ.

3.5 Stiffness degradation

Application of cyclic or repeated loading on the beam-column joint causes reduction in the stiffness of the joint. This reduction in stiffness can be assessed by calculating secant stiffness. The secant stiffness in each cycle was calculated as the slope of the line joining the maximum positive displacement point in the forward cycle and the maximum negative displacement point in the
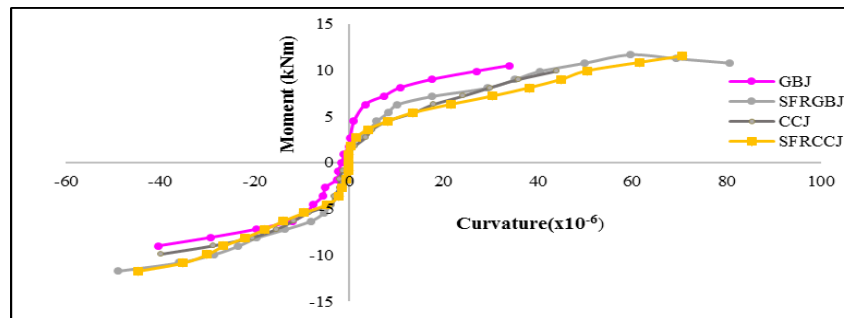
Fig. 9 Moment curvature plot

reverse cycle. The stiffness degradation of the specimens is shown in Fig. 8. From the Figure it may be noted that SFRGBJ exhibit the highest initial stiffness. It can also be seen that GBJ and SFRGBJ exhibit milder slope than CCJ and SFRCCJ specimens. Also it may be noted that the rate of reduction of stiffness is gradual in GBJ specimens than CCJ specimens.

3.6 Moment curvature relation

The moment curvature relation is related to the distribution of moments and the maximum value of strain in concrete. From the observed loads, moments were calculated according to the loading conditions at beam tip. Strains were measured using LVDTs attached to the top and bottom most fibers of beam. Curvature of the beam was calculated using Eq. (1)

$$\text{Curvature, } = \frac{\varepsilon_b + \varepsilon_t}{l} \tag{1}$$

Where ε_t is the strain at top fiber, ε_b is the strain at bottom fiber and l is the distance between top and bottom fiber.

The moment curvature plot obtained by plotting the corresponding moments and curvatures is shown in Fig. 9. It may be noted that the curve is linear up to the first crack moment and then onwards the joint shows non-linear behavior. It may be seen that the moment curvature envelope of GBJ and CCJ are comparable and GBJ exhibits more nonlinearity than CCJ specimens.

4. Conclusions

The load deflection characteristics, energy dissipation, ductility and stiffness degradation of plain and fiber reinforced beam column joints subjected to reverse cyclic loading were investigated in this study. The results indicated that the use of fibers could enhance the strength and ductility of beam column joints marginally. The experimental results lead to the following conclusions.
   • Behavior of plain and fiber reinforced geopolymer beam column joints are almost similar to that of conventional concrete beam column joints.
   • First crack load and ultimate load carrying capacity of GBJ and CCJ are almost the same.
   • Energy absorption capacity of GBJ and CCJ are almost the same in forward and backward loading cycles and increase in energy absorption capacity after each cycle showed a similar trend. Energy absorption capacity of GBJ is 39% higher than that of CCJ.

• The GBJ showed more ductile behavior than CCJ and the displacement ductility of GBJ was 1.47 times higher than that of CCJ.

The rate of degradation of stiffness is comparatively less and hence the GBJ member has sufficient capacity to resist reverse cyclic loading than CCJ member.

Acknowledgements

References

Al Bakri, M.M., Mohammed, H., Kamarudin, H., Niza, I.K. and Zarina, Y. (2011), "Review on fly ash-based geopolymer concrete without portland cement", *J. Eng. Tech. Res.*, **3**(1), 1-4.

Bakharev, T. (2005), "Geopolymeric materials prepared using class F fly ash and elevated temperature curing", *Cement Concrete Res.*, **35**(6), 1224-1232.

Dattatreya, J.K., Rajamane, N.P., Sabitha, D., Ambily, P.S. and Nataraja, M.C. (2011), "Flexural behaviour of reinforced geopolymer concrete beams", *J. Civil Struct. Eng.*, **2**(1), 138.

Ganesan, N., Indira, P.V. and Sabeena, M.V. (2014), "Behaviour of hybrid fibre reinforced concrete beam-column joints under reverse cyclic loads", *Mater. Des.*, **54**, 686-693.

Ganesan, N., Abraham, R. and Raj, S.D. (2015), "Durability characteristics of steel fibre reinforced geopolymer concrete", *Constr. Build. Mater.*, **93**, 471-476.

Ganesan, N., Ruby, A. and Deepa, R.S. (2015), "Durability characteristics of steel fiber reinforced geopolymer concrete", *Constr. Build. Mater.*, **93**, 471-476

Haach, V.G., El, A.L.H.D.C. and El Debs, M.K. (2008), "Evaluation of the influence of the column axial load on the behavior of monotonically loaded R/C exterior beam-column joints through numerical simulations", *Eng. Struct.*, **30**(4), 965-975.

Hardjito, D., Wallah, S.E., Sumajouw, D.M. and Rangan, B.V. (2004), "On the development of fly ash-based geopolymer concrete", *ACI Mater. J.-Am. Concrete Inst.*, **101**(6), 467-472.

IS 383 (1970) (Reaffirmed 2002), "Specifications for coarse and fine aggregate from natural sources for concrete", Code of Practice, 2nd Revision, BIS, New Delhi.

IS: 10262 (2009), "Recommended guidelines for concrete mix design"-Code of Practice, BIS, New Delhi.

IS: 12269 (1987) (Reaffirmed on 1999), "Specification for 53 grade ordinary Portland cement", Code of Practice, BIS, New Delhi.

Kannapiran, K., Sujatha, T. and Nagan, S. (2013), "Resistance of reinforced geopolymer concrete beams to acid and chloride migration", *Asian J. Civil Eng.*, **14**, 225-238.

Rangan, B.V. (2006), "Studies on low calcium fly ash based geopolymer concrete", *Indian Concrete J.*, 9-17.

Sarker, P.K. (2009), "Analysis of geopolymer concrete columns", *Mater. Struct.*, **42**(6), 715-724.

Sarker, P.K. (2011), "Bond strength of reinforcing steel embedded in fly ash-based geopolymer concrete", *Mater. Struct.*, **44**(5), 1021-1030.

Sujatha, T., Kannapiran, K. and Nagan, S. (2012), "Strength assessment of heat cured geopolymer concrete slender column", *Asian J. Civil Eng.*, **13**(5), 635-646.

CC